

# **CRYOGENIC DURABILITY OF A CARBON FIBER REINFORCED CYANATE ESTER COMPOSITE: DEGREE-OF- CURE EFFECT**

Daniel L. Polis, Marjorie F. Sovinski, Brian Harris, and Dave Puckett  
National Aeronautics and Space Administration  
Goddard Space Flight Center  
Greenbelt MD, 20771

Charles He, Robert Kiwak  
Swales Aerospace  
5050 Powder Mill Road  
Beltsville MD, 20705

## **ABSTRACT**

The James Webb Space Telescope (JWST) will be located approximately 1.5 million kilometers from Earth, producing extremely cold temperatures on the optical portion of the observatory. Specifically, the Optical Telescope Element (OTE) and Integrated Science Instrument Module (ISIM) will operate at approximately  $-240^{\circ}\text{C}$ . Construction of the structural components of the OTE and ISIM require bonding dissimilar materials together, e.g. Invar-36 (an iron-nickel alloy) to a carbon fiber reinforced cyanate ester composite (CFRCE) with an epoxy adhesive. While these materials enable the cryogenic stability required for optical performance, their joint strength at these extreme conditions presents a unique design challenge. Therefore, the current study presents a detailed investigation into the optimization of cryogenic composite durability. It is demonstrated that by controlling the degree-of-cure of a laminate, one can achieve an enhanced resistance to microcracking and an improved residual strength following cryogenic cycling to  $-253^{\circ}\text{C}$ .

**KEY WORDS:** Applications - Cryogenic, Carbon Fiber Composite, Microcracking/Crazing

# 1. INTRODUCTION

There has been a considerable amount of research focused on thermal cycling of composites and its effect on microcracking.(i) Much of this work explores the relationship between constituent types and ply orientations on microcracking. However, it is often the case that the constituent types are dictated by other governing requirements. For example, in many space structures stiffness requirements drive fiber type and ply orientation selection, while contamination requirements may drive resin selection. Therefore, studies which examine the impact of cure process parameters on thermal cycling stability/durability, such as that reported by Timmerman et. al.,(ii) provide an additional tool for satisfying the challenging design requirements in cryogenic composite applications.

Although microcracking is directly relevant to cryogenic liquid-storage systems,(iii) the performance of stable space structures is indirectly tied to microcracking through its effect on elastic and ultimate properties.(iv) To this end, this work explores the effect of a small number of extreme thermal cycles (25°C to -253°C) on the morphological changes and mechanical behaviors of a candidate laminate for the James Webb Space Telescope (JWST).

JWST will be located 1.5 million kilometers from Earth and shaded by its deployable sunshield will experience extremely cold temperatures on the optical portion of the observatory. The optical portion of the observatory will operate at approximately -240°C and must be able to survive temperatures near -253°C. JWST will not go through on-orbit cycling due to its stable position with respect to the Sun and Earth system (second Lagrange point). However, JWST's structural components will see a small number, <20, of ground-based test cycles followed by one cool down to the operating temperature following launch.

Construction of the structural components require bonding dissimilar materials together, such as Invar-36 (a low expansion iron-nickel alloy) to a carbon fiber reinforced cyanate ester matrix composite with an epoxy adhesive. While these materials enable the cryogenic stability required for optical performance, their joint strength at these extreme conditions presents a competing materials challenge. Furthermore, the joint strength at cryogenic temperatures is dominated by the interlaminar strength of the composites themselves. Therefore, this study describes the relationship between the degree-of-cure (DoC) of the composite and its interlaminar strength retention following thermal cycling between room temperature and cryogenic survival temperatures (-253°C). As a result, we seek to cryogenically condition the components on the ground to reach a more stable configuration on orbit.

## 2. EXPERIMENTAL

**2.1 Materials** Unidirectional pre-impregnated material (prepreg), referred to as M55J/954-6 tape, was purchased from Hexcel Corporation. The M55J fiber is an ultra high modulus polyacrylonitrile (PAN) based carbon fiber from Toray, with a tensile modulus ~ 540 GPa (78 Msi) and a tensile strength ~ 4,020 MPa (583 ksi). The 954-6 resin is a cyanate ester based

matrix, designed to cure at 121°C (250 °F).(v) The tow size was 6000. The nominal prepreg resin content and fiber areal weight were 30.5 weight% and 81.5 g/m<sup>2</sup>, respectively.

Four laminates, designated A, B, C, and D, were made to examine the effect of DoC. Laminates were made using a vacuum bag/autoclave process with a caul plate. The four laminates had equivalent layups of [[45/0<sub>3</sub>/-45/0<sub>2</sub>]<sub>S</sub>]<sub>3</sub>. Each laminate was ultrasonically inspected for quality assurance. The cure schedules for all the laminates are shown in Table 1, and were designed to achieve a range of cures between ~75 and 100%, based on previous work from individual plies cured in air at atmospheric pressure.(vi)

**Table 1:** Summary of laminate cure schedules

Laminate	Max 1st ramp rate (°C/min)	1st hold temperature°C (°F)	1st hold time (min)	Max 2nd ramp rate (°C/min)	2nd hold temperature°C (°F)	2nd hold time (min)	DoC (%)
A	2	126 (260)	135	-	-	-	77
B	2	126 (260)	180	-	-	-	81
C	2	126 (260)	180	2	149 (300)	120	89
D	2	126 (260)	180	2	176 (350)	120	95

**2.2 Characterization** Cure levels were determined with a TA Instruments Model 2910 differential scanning calorimeter (DSC), using as-received prepreg as the 100% uncured reference. The samples were tested in nitrogen and ramped at 20°C/min from room temperature to 375°C. The uncured reference was tested using hermetic pans, but the laminates were tested using open pans because of their size. A thermogravimetric method was used to determine the local resin content so the enthalpies measured with DSC could be normalized.(vii) Each sample was tested in triplicate and the three results averaged.

Composite glass transition temperatures ( $T_g$ ) were measured on a TA Instruments Model 2980 dynamic mechanical analyzer (DMA). Samples were run in a 3-point bending configuration and heated at a ramp rate of 2°C/min. The samples dimensions were 60mm x 6 mm x 3 mm. The samples were cut such that the y-direction of the laminates was coincident with the 60 mm dimension. The  $T_g$ 's were taken as the peak in the tan delta signal (loss modulus/storage modulus).

Thermal cycling was performed on all mechanical test specimens and microcrack specimens, which are described below. Samples were set unconstrained on a copper cold plate cooled with a cryocooler in vacuum. Silicon diodes, placed on representative specimens, were used to monitor actual sample temperatures. The specimens were ramped at <2°C/min from 25°C to -253°C and back to 25°C. The chamber was held at -253°C for 1 hour on each cycle to ensure that all samples fell within 5°C of the target temperature. Twenty cycles were performed on mechanical test specimens, whereas microcrack specimens were removed, inspected, and returned to the chamber in order to generate microcrack density versus cycle data.

Microcrack density determinations were performed on approximately 25 mm x 25 mm square laminates for the 0° and 45° specimens, respectively. Samples were polished and examined at 200x magnification on a Nikon Epiphot Metalograph. Cracks were only counted when they traversed through an entire ply. Four specimens from each laminate were evaluated, two cut parallel to the x-direction of the laminate and two cut at 45° to the x-direction. The samples cut

parallel to the x-direction were used to evaluate all of the 0° plies, whereas the samples cut at 45° were used to evaluate the 45° plies. Microcrack results are reported in average cracks/mm/ply for the 0° and 45° plies.

Flatwise tensile testing (viii) and short-beam shear (ix) were performed on an Instron 4400 test machine with a 44 kN (10,000 lb) capacity load cells. These tests were performed at both room temperature (~25°C) and submerged in liquid nitrogen (-196°C). Flatwise tensile specimens were 31.8 mm x 31.8 mm square specimens bonded to 25.4 mm x 25.4 mm blocks with Hysol EA9394 epoxy and cured at room temperature. The laminates were thermally cycled, as describe above, prior to bonding to the test blocks. For room temperature testing aluminum blocks were used, whereas Invar-36 blocks were used for testing at -196°C in order to more closely match the laminate thermal expansion. This configuration, with 3.2 mm overhang of the laminate, has been shown to yield a relatively uniform stress state over the 25.4 mm x 25.4 mm block areas at room temperature. Therefore the failure strengths can be accurately determined from the load divided by the bond area (P/A). In contrast, when the samples are tested at -196°C, finite element modeling reveals peaking on the order of ~25% above the average failure stress and shear stresses are no longer negligible.(x) However, P/A strengths are reported since it provides a good relative comparison between cure processes. Short-beam shear specimens were 18 mm x 6 mm x 3 mm with a nominal span of 12 mm. They were loaded at a rate of 1.27 mm/min.

### 3. RESULTS AND DISCUSSION

**3.1 Degree-of-cure** In order to explore the relationship between mechanical properties and processing, an attempt was made to produce a range of cure states through the processing routes outlined in Table 1. Table 1 also contains the measured DoC for each laminate. Figure 1 shows the  $T_g$  of these laminates versus the DoC. Plotted along with data from this study is the  $T_g$  versus DoC data from Georjon and Galy.(xi) Reasonable agreement is found between the commercially available prepreg system evaluated in this paper and the model system evaluated by Georjon and Galy, who examined the polymerization of the dicyanate of biphenol A, both catalyzed and uncatalyzed. Both studies reveal  $> 3^\circ\text{C}$  increase in  $T_g$  per 1% increase in DoC, making  $T_g$  a good candidate for process monitoring. Differences between our results versus that reported by Georjon and Galy may be attributed to  $T_g$  testing differences (ramp rate and DSC vs DMA) as well as chemistry. DoC is more difficult to measure on prepreg since fiber volume must also be determined, so this correlation could be useful in a manufacturing environment.

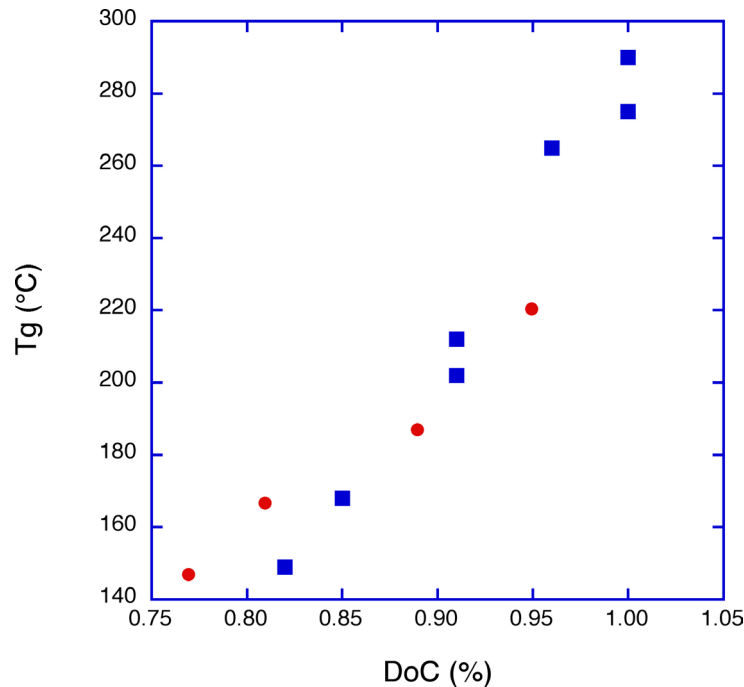


**Figure 1.** Glass transition temperature ( $T_g$ ) versus degree-of-cure (DoC) for the laminates in this study (red circles) along with laminates from Reference 11 (blue squares).

### 3.2 Microcrack density:

Microcracks are defined as planar cracks, which are oriented in a given ply such that the 2-direction (lamina coordinates) is normal to the crack plane. Thus, these cracks can propagate parallel to the fiber direction (1-direction) and perpendicular to the ply interface (3-direction). In this study, the cracks propagated in the 3-direction until they reached a cross ply, at which point they typically terminate. This is consistent with other studies.(1) Crack dimensions were not evaluated in the 1-direction. Microcracks were counted by examining each ply in the 1-3 plane. In other words, the 0° and 45° plies were assessed from different coupons so the plane of the microcracks would be normal to the image plane. An example of such a photomicrograph for a portion of a 45° ply is shown in Figure 2. Cracks were only counted if they traversed an entire ply. Crack densities are reported in average cracks/mm/ply for the 0° and 45° plies.



**Figure 2.** Photomicrograph showing 3 microcracks in a 45° ply. Cracks terminate at the 0° cross plies above and below the ply of interest.

Figures 3 and 4 show the average crack densities for the 0° and 45° plies from laminates A thru D. First, it is evident that the crack densities for the two orientations are not the same, which is expected due to the different levels of constraint for the 0° and 45°. Secondly, all the curves

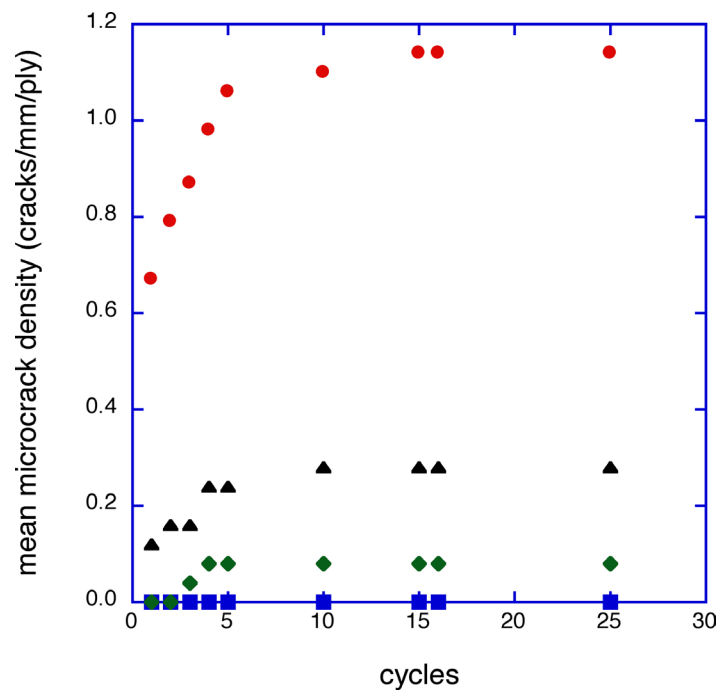


**Figure 3.** Average microcrack density for 0° plies versus the number of cryogenic cycles for laminates A (red circles), B (blue squares), C (green diamonds), and D (black triangles).

seem to suggest that most of the stress relief occurs in the first several cycles, ~5, followed by a more gradual increase in crack density. Finally, laminate B has the lowest 0° and 45° crack density, even though it had an intermediate DoC.

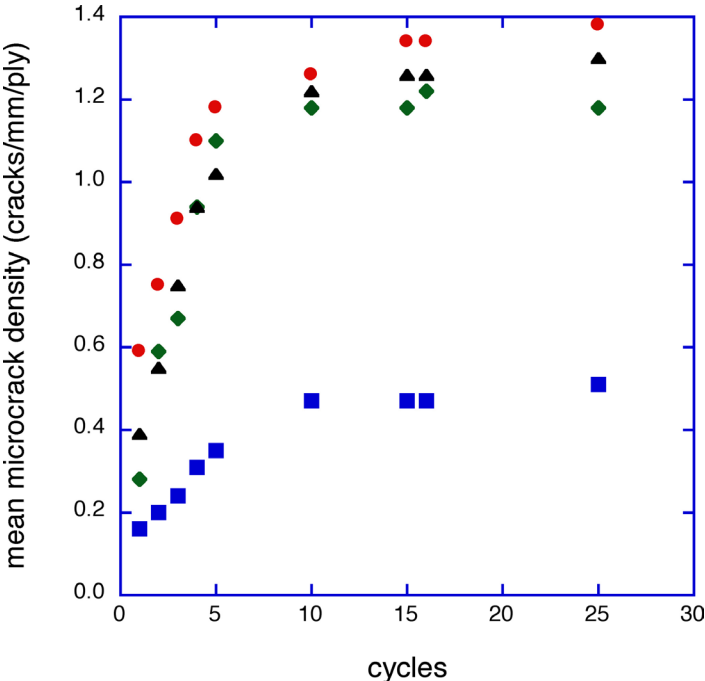


**Figure 4.** Average microcrack density for 45° plies versus the number of cryogenic cycles for laminates A (red circles), B (blue squares), C (green diamonds), and D (black triangles).

### 3.3 Mechanical testing:

Interlaminar strength, both tensile and shear, are key design properties at cryogenic temperatures and are most easily evaluated by flatwise tensile and short-beam shear testing. Figures 5 and 6 report the results of the tensile and shear tests, respectively, for both 25°C and -196°C. All the samples had been thermally conditioned prior to testing, as described in Section 2.2.

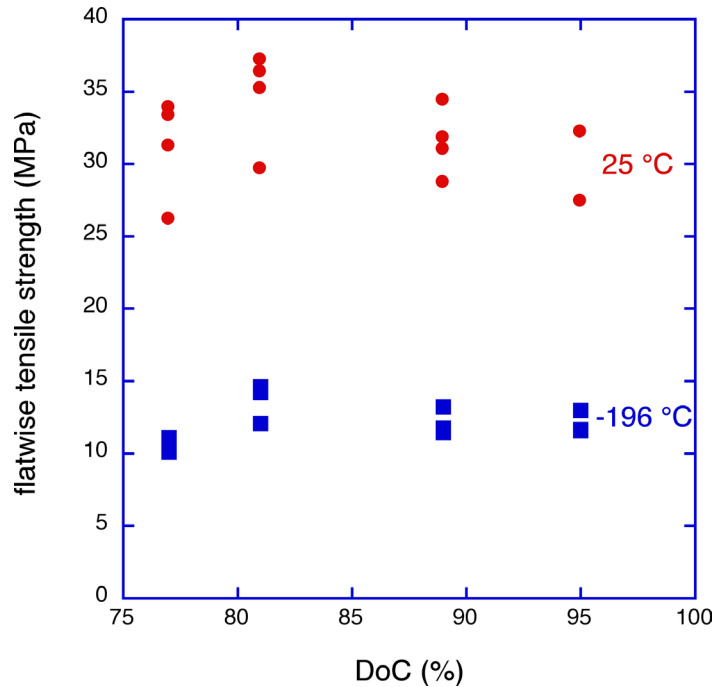


**Figure 5.** Flatwise tensile failure load at 25 °C (red circles) and -196°C (blue squares) versus degree-of-cure (DoC) for laminates following thermal cycling of the laminates.

The small sample size, as few as two in some groups, makes it difficult to draw statistically sound conclusions. In an attempt to increase the sample size at each cure level, the 25°C and -196°C data are combined by normalizing the individual results by the respective global averages. The global average is the average result from all the samples tested at a given temperature (25°C or -196°C) for a given test (shear or tension). Figures 7 and 8 show this normalized data for the flatwise tensile and short-beam shear tests.

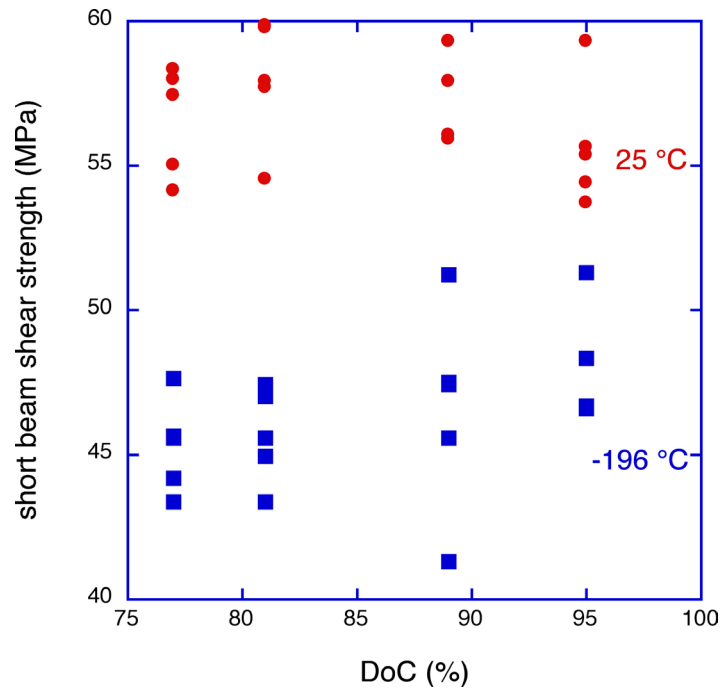


**Figure 6.** Short-beam shear strength at 25°C (red circles) and -196°C (blue squares) versus degree-of-cure (DoC) for laminates following thermal cycling of the laminates.

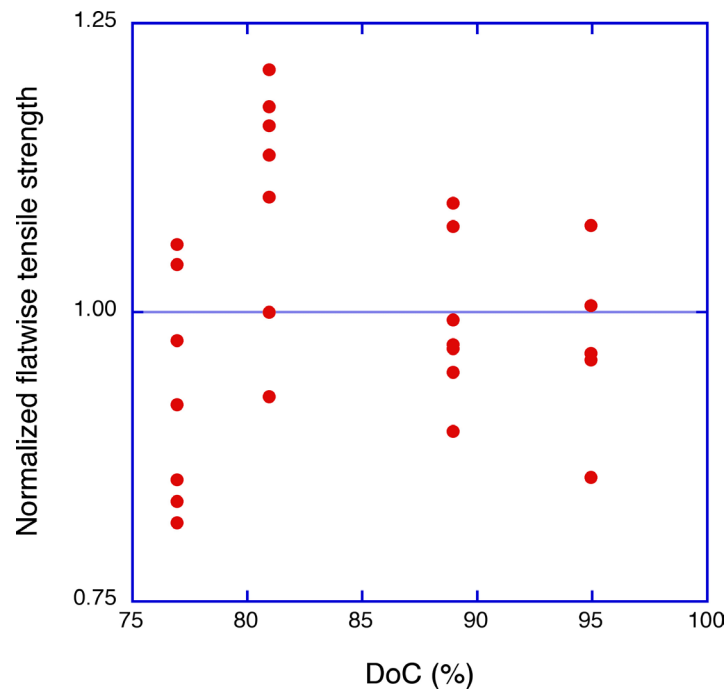


**Figure 7.** Normalized flatwise tensile strength from 25°C and -196°C testing versus degree-of-cure (DoC).

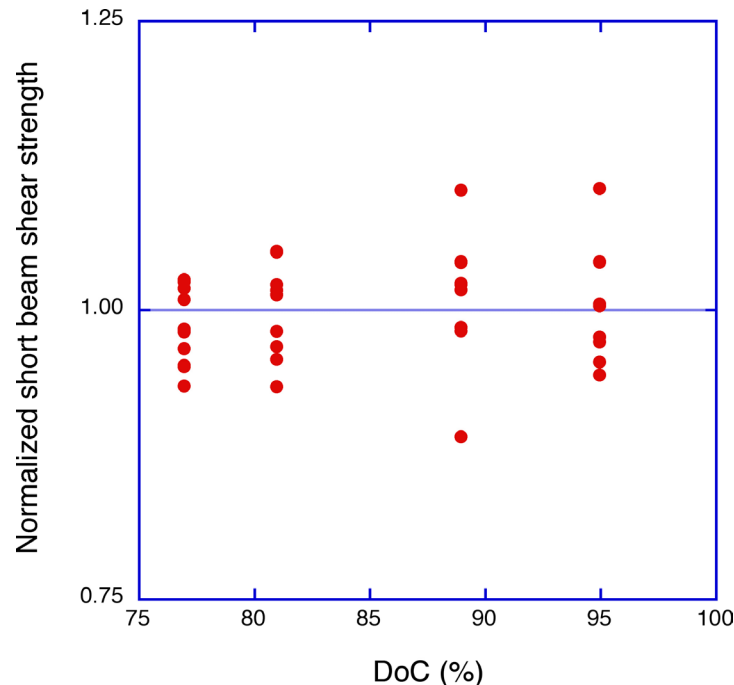


**Figure 8.** Normalized short-beam shear strength from 25°C and -196°C testing versus degree-of-cure (DoC).

This analysis reveals an improvement in flatwise tensile strength for laminate B, which has an intermediate DoC of 81%. Specifically, the mean normalized failure loads for laminates A thru D are 0.93, 1.10, 0.99, and 0.97, respectively. Based on the scatter in the data (pooled standard deviation = 0.09) this improvement in flatwise tensile strength for laminate B is statistically significant. In contrast, the short-beam shear strength data does not distinguish between the different DoC's. The mean normalized shear strengths for laminates A thru D are 0.98, 1.00, 1.01, and 1.01, respectively (pooled standard deviation = 0.05).

#### 4. CONCLUSIONS

The results of this study demonstrate that by controlling the degree-of-cure, one can optimize the cryogenic durability of carbon fiber reinforced cyanate ester composites. Specifically, an 81% DoC was superior to 77%, 89%, and 95% DoC. The 81% DoC laminate exhibited the lowest microcrack density and the highest flatwise tensile strength following thermal cycling between 25°C and -253°C. These results are summarized in Figure 9, which displays the flatwise tensile strength at -196°C and a cryogenic durability parameter defined as the inverse of the microcrack density. This durability parameter was determined from the average of cracks in all of the plies, both 0° and 45°, following 25 thermal cycles.

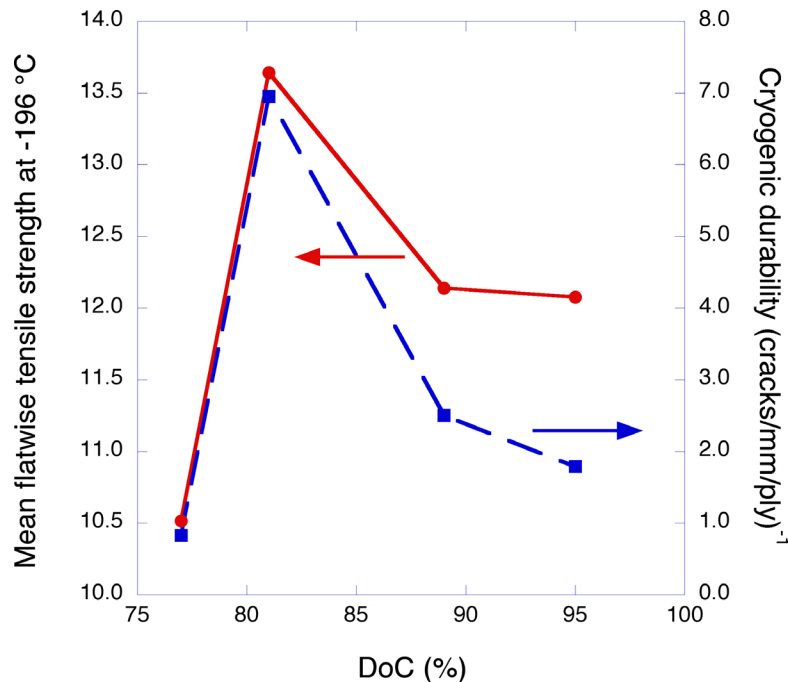


**Figure 9.** Mean flatwise tensile strength at -196°C (red circles) following twenty thermal cycles to -253°C and cryogenic durability (1/crack density) following twenty-five thermal cycles to -253°C versus DoC.

The occurrence of a maximum in both the mechanical and physical responses of the composites as a function of DoC indicate competing mechanisms. One possible origin is the competition between resin strength and residual stress from cure. Typically, it is expected that as the DoC progresses, crosslink density will increase and in turn increase the resin strength. However, the increase in DoC is also associated with an increase in  $T_g$ , which affects the resins ability to relax stress at a lower test temperature ( $T_{test}$ ), effectively increasing the stress free temperature ( $T_{stressfree}$ ). Therefore, at cryogenic temperatures, high DoC laminates may have high resin strengths, but they also have the high residual stresses from the larger ( $T_{test} - T_{stressfree}$ ). The balance between these factors could be the cause for the behavior observed in Figure 9. This competition provides a design parameter outside of constituent types and ply orientations, namely degree-of-cure, which can be used to improve the cryogenic performance of composites.

## 5. REFERENCES

- i. T. Brown, The Effect of Long-Term Thermal Cycling on the Microcracking Behavior and Dimensional Stability of Composite Materials. Thesis submitted to Virginia Polytechnic Institute and State University, VA, 1997, 247.
- ii. J.F. Timmerman, B.S. Hayes, and J.C. Seferis, Polymer Composites, **24** (1), 132 (2003).
- iii. D.R. Ambur et. al., AIAA/ASME/ASCE/AHS/ASC 37th Structures, Structural Dynamics, and Materials Conference, Salt Lake City, UT (1996).

---

iv. D. Bashford and D. Eaton, Proceedings of the Conference on Spacecraft Structures, Materials and Mechanical Testing, The Netherlands, 1996, pp. 513-520.

v. 954-6 Product Data Sheet, Hexcel Corporation, Pleasanton, CA, 2000.

vi. R.W. Jones, et. al. in D.O. Thompson and Dale E. Chimenti, eds., Proceedings of the Review of Progress in Quantitative Nondestructive Evaluation, American Institute of Physics, Melville, NY, 2005, pp 1094-1099.

vii. D.L. Polis and M.F. Sovinski, Submitted as NASA Technical Memorandum, 2005.

viii. ASTM C 297, " Standard Test Method for Flatwise Tensile Strength of Sandwich Constructions," ASTM International.

ix. ASTM D 2344, "Standard Test Method for Short-Beam Strength of Polymer Matrix Composite Materials and Their Laminates," ASTM International.

x. A. Bartoszyk, et. al., SPIE Symposium on Optics & Photonics, San Diego, CA (2005).

xi. O. Georjon and J. Galy, Journal of Applied Polymer Science, 65, 2471 (1997).